



Detecting a Higgs Pseudoscalar with a Z Boson at the LHC

Chung Kao^{a*}, Geoffrey Lovelace^{a†} and Lynne H. Orr^{b‡}

^a*Department of Physics and Astronomy, University of Oklahoma, Norman, OK 73019*

^b*Department of Physics and Astronomy, University of Rochester, Rochester, NY 14627*

Abstract

We have adopted two Higgs doublet models to study the production of a Higgs pseudoscalar (A^0) in association with a Z gauge boson from gluon fusion ($gg \rightarrow ZA^0$) at the CERN Large Hadron Collider. The prospects for the discovery of $Z A^0 \rightarrow \ell \bar{\ell} b \bar{b}$ are investigated with physics backgrounds and realistic cuts. Promising results are found for $m_A \lesssim 260$ GeV in two Higgs doublet models when the heavier Higgs scalar (H^0) can decay into a Z boson and a Higgs pseudoscalar (A^0). Although the cross section of $gg \rightarrow ZA^0$ is usually small in the minimal supersymmetric standard model, it can be significantly enhanced in general two Higgs doublet models. This discovery channel might provide an opportunity to search for a Higgs scalar and a Higgs pseudoscalar simultaneously at the LHC and could lead to new physics beyond the Standard Model and the minimal supersymmetric model.

Typeset using REVTeX

*E-mail address: Kao@physics.ou.edu

†Present address: Department of Physics, California Institute of Technology, Pasadena, CA 91125.

‡E-mail address: Orr@pas.rochester.edu

I. INTRODUCTION

The Standard Model has been very successful in explaining most experimental data to date, culminating in the discovery of the top quark [1] and the evidence of the tau neutrino [2]. One of the most important experimental goals for Run II of the Fermilab Tevatron and the CERN Large Hadron Collider (LHC) is the experimental investigation of the mechanism behind electroweak symmetry breaking—the discovery of the Higgs bosons or the proof of their non-existence, and the search for higher symmetries beyond the Standard Model.

In the Standard Model (SM), the Higgs mechanism requires only one Higgs doublet to generate masses for fermions and gauge bosons. It leads to the appearance of a neutral CP-even Higgs scalar after electroweak symmetry breaking (EWSB). The LEP2 experiments have established a lower bound of 114.4 GeV [3] for the SM Higgs boson mass at the 95% confidence level.

A general two Higgs doublet model (2HDM) [4] has Higgs doublets with the vacuum expectation values v_1 and v_2 that are needed to give masses to both down-type and up-type quarks as well as leptons and gauge bosons. There are five physical Higgs bosons: a pair of singly charged Higgs bosons H^\pm , two neutral CP-even scalars H^0 (heavier) and h^0 (lighter), and a neutral CP-odd pseudoscalar A^0 . At the tree level, the couplings of the Higgs bosons to fermions and gauge bosons are determined by six independent parameters: the four Higgs boson masses, the ratio of vacuum expectation values $\tan\beta \equiv v_2/v_1$, and a mixing angle α_H between the weak and mass eigenstates of the neutral scalars.

The minimal supersymmetric standard model (MSSM) [5] requires two Higgs doublets to generate masses for fermions and gauge bosons and to cancel triangle anomalies associated with the fermionic partners of the Higgs bosons. At the tree level, the Higgs sector has only two free parameters that are commonly selected to be m_A and $\tan\beta$. The mixing angle α_H between the neutral scalars is often chosen to be negative ($-\pi/2 \leq \alpha_H \leq 0$). The LEP2 collaborations have set a lower bound of 91 GeV and 91.9 GeV [6] for the m_h and the m_A , respectively.

Extensive studies have been made for the detection of the heavier MSSM Higgs bosons (H^0 and A^0) at the CERN LHC [7–16]. For $\tan\beta \lesssim 5$, $A^0 \rightarrow \gamma\gamma$, $H^0 \rightarrow ZZ$ or $ZZ^* \rightarrow 4l$, and $A^0, H^0 \rightarrow t\bar{t}$ are possible discovery channels. The detection modes $A^0 \rightarrow Zh^0 \rightarrow l^+l^-\tau\bar{\tau}$ [11] or $l^+l^-\bar{b}\bar{b}$ [11,14,16] and $H^0 \rightarrow h^0h^0 \rightarrow b\bar{b}\gamma\gamma$ [16] may be promising channels for simultaneous discovery of two Higgs bosons in the MSSM. For large values of $\tan\beta$, the $\tau\bar{\tau}$ decay mode [9,14–16] and the muon pair decay mode [12–14,16] are promising discovery channels for the A^0 and the H^0 . In some regions of parameter space, the rates for Higgs boson decays to neutralinos ($H^0, A^0 \rightarrow \chi_2^0\chi_2^0$) are dominant and they might open up new promising modes for Higgs detection [10].

In two Higgs doublet models, there are two complementary channels to search for a Higgs scalar and a Higgs pseudoscalar simultaneously: (i) $A^0 \rightarrow Zh^0$ [11,14,16] with a coupling proportional to $\cos(\beta - \alpha_H)$ and (ii) $H^0 \rightarrow ZA^0$ with a coupling proportional to $\sin(\beta - \alpha_H)$. At the LHC with high energy, the fraction x of the parton momentum to the initial proton momentum can become small and greatly enhance the gluon-gluon luminosity. Therefore, gluon fusion can be a significant source of producing a Higgs pseudoscalar (A^0) and a Z boson ($gg \rightarrow ZA^0$) via triangle and box diagrams with the third generation quarks [17,18].

In this article, we present the prospects of discovering a Higgs pseudoscalar (A^0) associated with a Z boson produced at the LHC followed by $Z \rightarrow \ell\bar{\ell}$ and $A^0 \rightarrow b\bar{b}$. We evaluate the cross section for the Higgs signal and the complete SM background $pp \rightarrow \ell\bar{\ell}b\bar{b} + X$ with realistic cuts and study the discovery potential at the LHC. The production cross sections of ZA^0 at the LHC in a two Higgs doublet model and the MSSM are discussed in Section II. The dominant physics backgrounds from production of $\ell\bar{\ell}b\bar{b}$ and $W^+W^-b\bar{b}$ are presented in Section III. The observability of $ZA^0 \rightarrow \ell\bar{\ell}b\bar{b}$ is discussed in Section IV. Conclusions are drawn in Section V.

II. THE PRODUCTION CROSS SECTIONS

We calculate the cross section for $pp \rightarrow ZA^0 + X$ via $gg \rightarrow ZA^0$ within the framework of two Higgs doublet models (2HDM) with Model II of the Yukawa interactions for Higgs bosons and fermions [19]. In Model II of 2HDMs and the MSSM, one Higgs doublet (ϕ_1) couples to down-type quarks and charged leptons while another doublet (ϕ_2) couples to up-type quarks and neutrinos.

The production of ZA^0 from gluon fusion involves triangle and box diagrams with loop integrals that are expressible in terms of the Spence functions [20,21]. In our analysis, the one loop integrals were evaluated numerically with a FORTRAN code developed for one-loop diagrams [22]. The parton distribution functions of CTEQ6L1 [23] are employed to evaluate the cross section for $pp \rightarrow ZA^0 \rightarrow \ell\bar{\ell}b\bar{b} + X$ with the Higgs production cross section $\sigma(pp \rightarrow ZA^0 + X)$ multiplied by the branching fractions of $Z \rightarrow \ell\bar{\ell}$ and $A^0 \rightarrow b\bar{b}$.

In Figure 1, we present the cross section $pp \rightarrow ZA^0 \rightarrow \ell\bar{\ell}b\bar{b} + X$ as a function of $\tan\beta$ in (a) the minimal supersymmetric model and (b) a two Higgs doublet model with $M_H = m_A + 100$ GeV, $m_h = 120$ GeV, and $\alpha_H = -\pi/4$. It is clear that the cross section in a 2HDM can be significantly larger than that in the the MSSM. Since M_H , m_h and α_H are free parameters in a 2HDM, the H^0 can decay into ZA^0 with $m_H > m_A + M_Z$. In the MSSM with $\tan\beta \gtrsim 10$, m_A and m_h are very close to each other for $m_A \lesssim 125$ GeV, while m_A and m_H are almost degenerate when $m_A \gtrsim 125$ GeV [12]. Therefore, the decay $H^0 \rightarrow ZA^0$ is kinematically inaccessible.

The cross section for $pp \rightarrow ZA^0 + X \rightarrow \ell\bar{\ell}b\bar{b} + X$ is shown in Figure 2 as a function of the Higgs scalar mixing angle α_H , in a two Higgs doublet model for $\tan\beta = 2, 10$, and 40 , and (a) $m_A = 150$ GeV and (b) $m_A = 400$ GeV. Also shown are the cross sections in the MSSM for $\tan\beta = 2$ (diamond), 10 (square), and 40 (circle). For $\alpha_H < 0$, the cross section in a 2HDM is significantly larger than that in the MSSM except when $\alpha_H \sim -\pi/2$. For $m_A > 250$ GeV and $\tan\beta \lesssim 7$, the branching fraction of $A^0 \rightarrow b\bar{b}$ is greatly suppressed when the Higgs pseudoscalar decays dominantly into $t\bar{t}$ with one of the top quarks being virtual.

We note that there are dips in Figures 1 and 2. For some values of $\tan\beta$ and α_H , the cross section of ZA^0 from gluon fusion is highly suppressed by the destructive interference between the triangle and the box diagrams as well as the negative interference between the top quark and the bottom quark loops, especially when they are comparable [17].

III. THE PHYSICS BACKGROUND

The dominant physics backgrounds to the final state of $Z A^0 \rightarrow \ell \bar{\ell} b \bar{b}$ come from $gg \rightarrow \ell \bar{\ell} b \bar{b}$ and $q \bar{q} \rightarrow \ell \bar{\ell} b \bar{b}$, $\ell = e$ or μ . The background from $pp \rightarrow W^+ W^- b \bar{b} + X$ (including $pp \rightarrow t \bar{t} + X$) followed by the decays of $W^\pm \rightarrow \ell^\pm \nu_\ell$, can be effectively reduced with cuts on the invariant mass of lepton pairs and the missing transverse energy. We have also considered backgrounds from $pp \rightarrow \ell \bar{\ell} g b + X$, $pp \rightarrow \ell \bar{\ell} g \bar{b} + X$, $pp \rightarrow \ell \bar{\ell} g q + X$, $pp \rightarrow \ell \bar{\ell} g \bar{q} + X$, and $pp \rightarrow \ell \bar{\ell} j j + X$, where $q = u, d, s$, or c and $j = g, q$ or \bar{q} .

Our acceptance cuts and efficiencies of b -tagging and mistagging are similar to those of the ATLAS collaboration [16]. In each event, two isolated leptons are required to have $p_T(\ell) > 15$ GeV and $|\eta(\ell)| < 2.5$. For an integrated luminosity (L) of 30 fb^{-1} , we require $p_T(b, j) > 15$ GeV and $|\eta(b, j)| < 2.5$. The b -tagging efficiency (ϵ_b) is taken to be 60%, the probability that a c -jet is mistagged as a b -jet (ϵ_c) is 10%, and the probability that any other jet is mistagged as a b -jet (ϵ_j) is taken to be 1%. Furthermore, we require the invariant mass of the opposite sign pair of leptons to be within 10 GeV of M_Z , that is $|M_{\ell\ell} - M_Z| \leq 10$ GeV.

For a higher integrated luminosity of 300 fb^{-1} , we require the same acceptance cuts as those for $L = 30 \text{ fb}^{-1}$, except $p_T(\ell) > 25$ GeV and $p_T(b, j) > 30$ GeV. The b -tagging efficiency (ϵ_b) is taken to be 50%, and the probability that a c -jet is mistagged as a b -jet (ϵ_c) is 14%.

In addition, we require that the missing transverse energy (\cancel{E}_T) in each event should be less than 20 GeV for $L = 30 \text{ fb}^{-1}$ and less than 40 GeV for $L = 300 \text{ fb}^{-1}$. This cut effectively reduces the background from $pp \rightarrow W^+ W^- b \bar{b} + X$ which receives the major contribution from both real and virtual top quarks $pp \rightarrow t^* \bar{t}^* + X$.

We have employed the programs MADGRAPH [24] and HELAS [25] to evaluate the background cross sections of $pp \rightarrow \ell \bar{\ell} b \bar{b} + X$, $\ell \bar{\ell} j j + X$, and $W^+ W^- b \bar{b} + X$. The $p_T(b, j)$ cut is effective in removing most of the SM background, while most b and \bar{b} from the Higgs decays pass the p_T cut.

In Figure 3, we present distributions for the transverse momenta (p_T) of leptons and bottom quarks for $pp \rightarrow Z A^0 \rightarrow \ell \bar{\ell} b \bar{b} + X$ and for the SM background of $pp \rightarrow \ell \bar{\ell} b \bar{b} + X$ via $gg \rightarrow \ell \bar{\ell} b \bar{b}$ and $q \bar{q} \rightarrow \ell \bar{\ell} b \bar{b}$. It is clear that the p_T cuts on leptons and bottom quarks are effective in removing most of the SM background, while most leptons from the Z decays and most b 's from the Higgs decays survive the p_T cuts.

IV. THE DISCOVERY POTENTIAL AT THE LHC

To study the discovery potential of $pp \rightarrow Z A^0 \rightarrow \ell \bar{\ell} b \bar{b} + X$ at the LHC, we calculate the background from the SM processes of $pp \rightarrow \ell \bar{\ell} b \bar{b} + X$ in the mass window of $m_A \pm \Delta M_{b\bar{b}}$ with $\Delta M_{b\bar{b}} = 22$ GeV.

We consider the Higgs signal to be observable if the $N\sigma$ lower limit on the signal plus background is larger than the corresponding upper limit on the background [7,26], namely,

$$L(\sigma_S + \sigma_B) - N\sqrt{L(\sigma_S + \sigma_B)} > L\sigma_B + N\sqrt{L\sigma_B} \quad (1)$$

which corresponds to

$$\sigma_S > \frac{N^2}{L} \left[1 + 2\sqrt{L\sigma_B}/N \right]. \quad (2)$$

Here L is the integrated luminosity, σ_S is the cross section of the Higgs signal, and σ_B is the background cross section within a bin of width $\pm\Delta M_{b\bar{b}}$ centered at m_A . In this convention, $N = 2.5$ corresponds to a 5σ signal.

We show the cross section with acceptance cuts in Figure 4 for $pp \rightarrow ZA^0 \rightarrow \ell\ell b\bar{b} + X$ in a 2HDM with $M_H = m_A + 100$ GeV, $m_h = 120$ GeV, and $\alpha_H = -\pi/4$ for an integrated luminosity of 30 fb^{-1} and a higher luminosity of 300 fb^{-1} . The curves for the 5σ and 3σ cross sections for the $Z A^0$ signal are also presented.

With a luminosity of 30 fb^{-1} , it is possible to establish a 3σ signal of $Z A^0 \rightarrow \ell\ell b\bar{b}$ for $m_A \lesssim 200$ GeV and $\tan\beta$ close to 2. At a higher luminosity of 300 fb^{-1} the discovery potential of this channel is greatly improved for $m_A \lesssim 250$ GeV.

In Tables I and II, we present event rates after acceptance cuts for the signal (N_S) and the background (N_B) as well as the ratio of signal to background N_S/N_B and $N_S/\sqrt{N_B}$ in a two Higgs doublet model with $\tan\beta = 2$, $\alpha_H = -\pi/4$. It is clear that our acceptance cuts can effectively reduce the physics background so that the ratio N_S/N_B is larger than 5% for $M_A \lesssim 250$ GeV. These data demonstrate that our statistical argument in Eq. (2) is valid in determining the signal observability.

TABLE I. Event rates after acceptance cuts for the signal (N_S) and the background (N_B) as well as the ratio of signal to background N_S/N_B and $N_S/\sqrt{N_B}$ in a two Higgs doublet model with $\tan\beta = 2$, $\alpha_H = -\pi/4$, and $m_H = m_A + 100$ GeV for an integrated luminosity of 30 fb^{-1} .

m_A (GeV)	N_S	N_B	N_S/N_B	$N_S/\sqrt{N_B}$
100	690	9939	1/14	6.9
150	252	4218	1/17	3.9
200	387	1950	1/5	8.8
250	50	978	1/19	1.6
300	6	525	1/88	0.3
350	1	299	1/360	0.05

TABLE II. The same as in Table I, except that the integrated luminosity is 300 fb^{-1} .

m_A (GeV)	N_S	N_B	N_S/N_B	$N_S/\sqrt{N_B}$
100	2821	22527	1/8	19
150	1234	13461	1/11	11
200	2062	7344	1/3.6	24
250	276	4152	1/15	4.3
300	33	2435	1/73	0.7
350	5	1483	1/310	0.1

V. CONCLUSIONS

We have found promising results for $pp \rightarrow ZA^0 \rightarrow \ell\bar{\ell}b\bar{b} + X$ via $gg \rightarrow ZA^0$ in two Higgs doublet models at the LHC with $L = 300 \text{ fb}^{-1}$ for $m_A \lesssim 260 \text{ GeV}$, $M_H = m_A + 100 \text{ GeV}$ and $\tan \beta \sim 2$. The physics background in the Standard Model can be greatly reduced with suitable acceptance cuts.

In the MSSM with $m_A \gtrsim 125 \text{ GeV}$, $m_A \sim m_H$, and the production cross section of $gg \rightarrow ZA^0$ is usually small. The production rate of $Z A^0$ from gluon fusion at the LHC is highly suppressed owing to the destructive interference between the triangle and the box diagrams as well as the negative interference between the top quark and the bottom quark loops, especially when they are comparable [17].

In a two Higgs doublet model, the cross section of $gg \rightarrow ZA^0$ can be greatly enhanced when the heavier scalar can decay into the pseudoscalar and a Z boson. If we take $m_H \sim m_A$ in a 2HDM, the Higgs signal will be reduced to the level of the MSSM. This discovery channel might lead to new physics beyond the Standard Model and the minimal supersymmetric model. Furthermore, we might be able to discover two Higgs bosons simultaneously if the heavier Higgs scalar (H^0) can decay into a Z boson and a Higgs pseudoscalar (A^0).

ACKNOWLEDGMENTS

This research was supported in part by the U.S. Department of Energy under grants No. DE-FG03-98ER41066, No. DE-FG02-03ER46040, and No. DE-FG02-91ER40685.

REFERENCES

- [1] CDF collaboration: F. Abe *et al.*, Phys. Rev. Lett. **74**, 2626 (1995); D \emptyset collaboration: S. Abachi *et al.*, Phys. Rev. Lett. **74**, 2632 (1995).
- [2] M. Nakamura [DONUT Collaboration], Nucl. Phys. Proc. Suppl. **77**, 259 (1999).
- [3] The LEP Higgs working group, <http://lephiggs.web.cern.ch/LEPHIGGS/www/>; LHWG note 2002-01.
- [4] J. Gunion, H. Haber, G. Kane and S. Dawson, *The Higgs Hunter's Guide* (Addison-Wesley, Redwood City, CA, 1990).
- [5] H.P. Nilles, Phys. Rep. **110** (1984) 1; H. Haber and G. Kane, Phys. Rep. **117** (1985) 75.
- [6] The LEP Higgs working group, <http://lephiggs.web.cern.ch/LEPHIGGS/www/>; LHWG note 2001-04.
- [7] H. Baer, M. Bisset, C. Kao and X. Tata, Phys. Rev. D **46**, 1067 (1992).
- [8] V. D. Barger, M. S. Berger, A. L. Stange and R. J. Phillips, Phys. Rev. D **45**, 4128 (1992); J. F. Gunion, R. Bork, H. E. Haber and A. Seiden, Phys. Rev. D **46**, 2040 (1992); J. F. Gunion and L. H. Orr, Phys. Rev. D **46**, 2052 (1992); J. F. Gunion, H. E. Haber and C. Kao, Phys. Rev. D **46**, 2907 (1992).
- [9] Z. Kunszt and F. Zwirner, Nucl. Phys. B **385**, 3 (1992).
- [10] H. Baer, M. Bisset, D. Dicus, C. Kao and X. Tata, Phys. Rev. D **47**, 1062 (1993); H. Baer, M. Bisset, C. Kao and X. Tata, Phys. Rev. D **50**, 316 (1994).
- [11] H. Baer, C. Kao and X. Tata, Phys. Lett. B **303**, 284 (1993); S. Abdullin, H. Baer, C. Kao, N. Stepanov and X. Tata, Phys. Rev. D **54**, 6728 (1996).
- [12] C. Kao and N. Stepanov, Phys. Rev. D **52**, 5025 (1995).
- [13] S. Dawson, D. Dicus and C. Kao, Phys. Lett. B **545**, 132 (2002).
- [14] CMS Technical Proposal, CERN/LHCC 94-38 (1994).
- [15] Atlas Technical Proposal, CERN/LHCC 94-43 (1994).
- [16] E. Richter-Was, D. Froidevaux, F. Gianotti, L. Poggioli, D. Cavalli and S. Resconi, Int. J. Mod. Phys. A **13**, 1371 (1998); ATLAS Detector and Physics Performance Technical Design Report, CERN/LHCC 99-14/15 (1999).
- [17] C. Kao, Phys. Rev. D **46**, 4907 (1992).
- [18] J. Yin, W. G. Ma, R. Y. Zhang and H. S. Hou, Phys. Rev. D **66**, 095008 (2002).
- [19] J. F. Donoghue and L. F. Li, Phys. Rev. D **19**, 945 (1979); L. J. Hall and M. B. Wise, Nucl. Phys. B **187**, 397 (1981).
- [20] G. 't Hooft and M. J. Veltman, Nucl. Phys. B **153**, 365 (1979).
- [21] G. Passarino and M. J. Veltman, Nucl. Phys. B **160**, 151 (1979).
- [22] C. Kao and D. A. Dicus, LOOP, a FORTRAN program for evaluating loop integrals based on the results in Refs. [20] and [21].
- [23] J. Pumplin, D. R. Stump, J. Huston, H. L. Lai, P. Nadolsky and W. K. Tung, JHEP **0207**, 012 (2002) [arXiv:hep-ph/0201195].
- [24] MADGRAPH, by T. Stelzer and W.F. Long, Comput. Phys. Commun. **81**, 357 (1994).
- [25] HELAS, by H. Murayama, I. Watanabe and K. Hagiwara, KEK report KEK-91-11 (1992).
- [26] N. Brown, Z. Phys. **C49** (1991) 657.

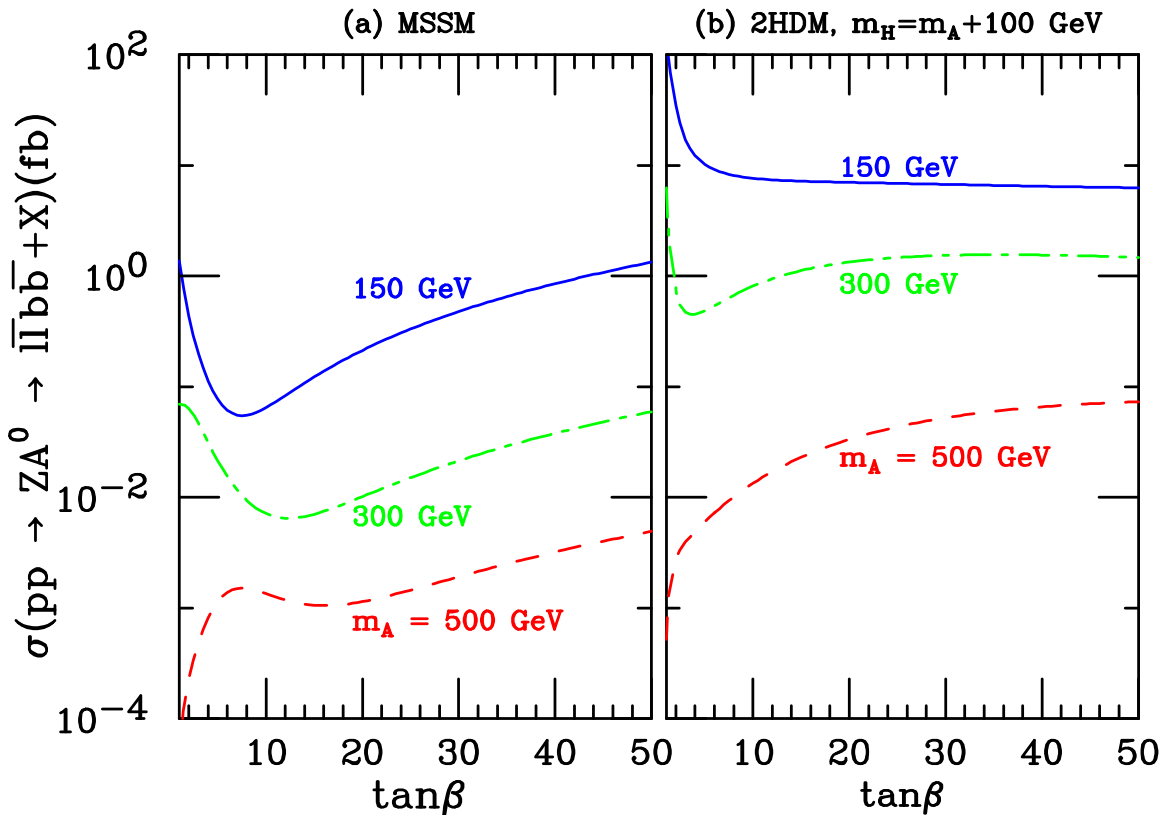


FIG. 1. The cross section for $pp \rightarrow ZA^0 + X \rightarrow \ell\bar{\ell}b\bar{b} + X$ in fb without cuts at $\sqrt{s} = 14$ TeV, as a function of $\tan \beta$, for $m_A = 150, 300$, and 500 GeV, in (a) the MSSM with $m_{\tilde{q}} = m_{\tilde{g}} = \mu = 1$ TeV, as well as in (b) a two Higgs doublet model with $M_h = 120$ GeV, $M_H = m_A + 100$ GeV and the Higgs mixing angle $\alpha_H = -\pi/4$.

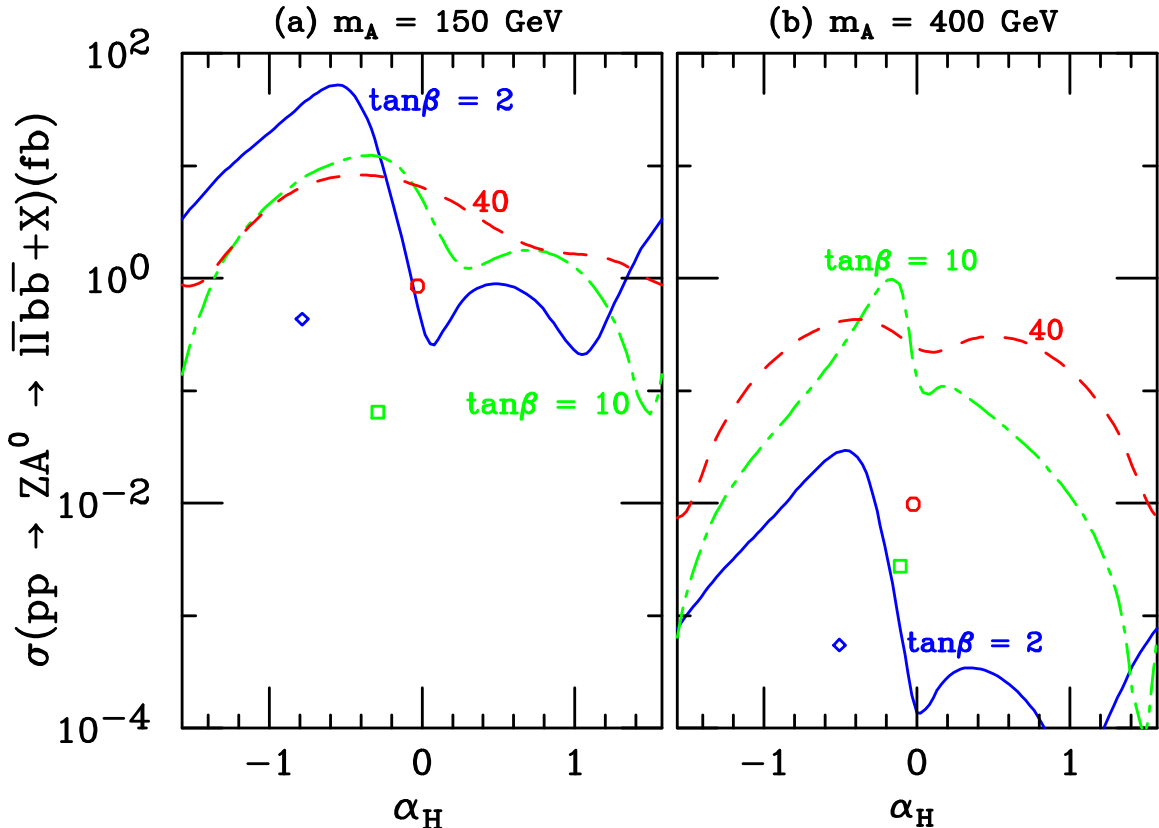


FIG. 2. The cross section for $pp \rightarrow ZA^0 + X \rightarrow \ell\bar{\ell}b\bar{b} + X$ in fb without cuts at $\sqrt{s} = 14$ TeV, as a function of the Higgs scalar mixing angle α_H , in a two Higgs doublet model with $M_h = 120$ GeV, $M_H = m_A + 100$ GeV for $\tan\beta = 2, 10$, and 40 , and (a) $m_A = 150$ GeV and (b) $m_A = 400$ GeV. Also shown are the cross sections in the MSSM for $\tan\beta = 2$ (diamond), 10 (square), and 40 (circle).

2HDM, $M_A = 150$ GeV, $\tan\beta = 40$

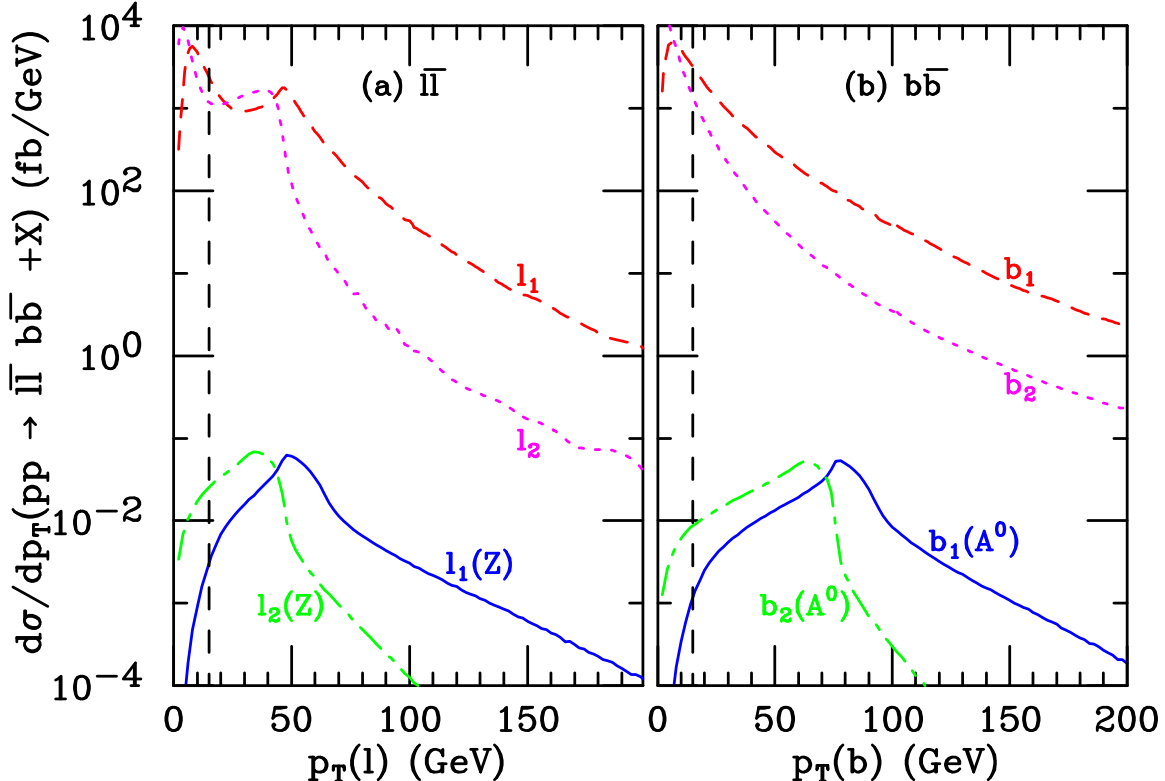


FIG. 3. The p_T distributions of leptons and bottom quarks in fb/GeV for $pp \rightarrow Z A^0 \rightarrow \ell\ell b\bar{b} + X$ (solid and dot-dashed) in a two Higgs doublet model with $m_A = 150$ GeV, $m_h = 120$ GeV, $m_H = m_A + 100$ GeV, the Higgs scalar mixing angle $\alpha = -\pi/4$, and $\tan\beta = 40$. We have chosen ℓ_1 or b_1 to be the lepton or the b quark with higher transverse momentum. Also shown is the contribution from the SM background of $pp \rightarrow \ell\ell b\bar{b} + X$ (dashed and dotted) via $gg \rightarrow \ell\ell b\bar{b}$ and $q\bar{q} \rightarrow \ell\ell b\bar{b}$. The p_T cuts remove events to the left of the vertical dashed line.

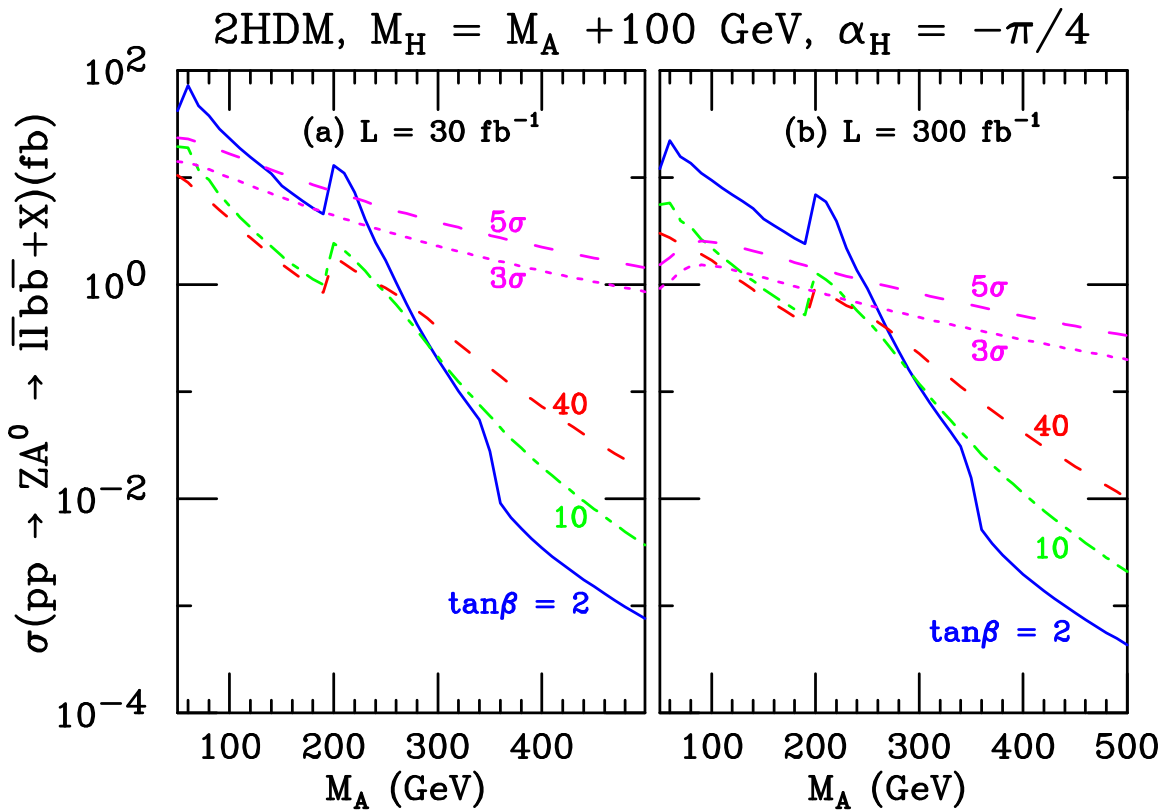


FIG. 4. The cross section in fb of $pp \rightarrow ZA^0 + X \rightarrow \ell\bar{\ell}b\bar{b} + X$ versus m_A , at $\sqrt{s} = 14$ TeV, in a two Higgs doublet model with $m_h = 120$ GeV, $m_H = m_A + 100$ GeV and the Higgs scalar mixing angle $\alpha_H = -\pi/4$, for $\tan\beta = 2$ (solid), 10 (dot-dashed), and 40 (dashed). Also shown are the 5σ (dashed) and 3σ (dotted) cross sections for the ZA^0 signal required for an integrated luminosity (L) of (a) 30 fb^{-1} and (b) 300 fb^{-1} . We have applied the acceptance cuts as well as the tagging and mistagging efficiencies described in the text.